Normal movement-selectivity in autism
supplementary materials

Ilan Dinstein[1], Cibu Thomas[3], Kate Humphreys[3], Nancy Minshew[4],
Marlene Behrmann[3], David J. Heeger[2,1]

[1] Center for Neural Science, New York University, 4 Washington Place, New York, New York, USA 10003.

[2] Department of Psychology, New York University, 6 Washington Place, New York, New York, USA 10003.

[3] Department of Psychology, Baker Hall, Carnegie Mellon University, Pittsburgh, Pennsylvania, USA 15213.

[4] Department of Neurology, University of Pittsburgh, 3471 Fifth Avenue, Pittsburgh, Pennsylvania, USA 15213.

Inventory:

7 Supplementary Figures:

Supplementary Figure 1 is related to Main Figures 1 and 2

Supplementary Figure 2 is related to Main Figure 3

Supplementary Figure 3 is related to Main Figure 4

Supplementary Figure 4 is related to Main Figure 6

Supplementary Figure 5 is related to Main Figure 7

Supplementary Figure 6 shows an additional analysis not necessarily related to a particular figure in the main text.

Supplementary Figure 7 is related to Main Figures 5-7

2 Supplementary Tables:

Supplementary Table 1 provides additional information about subjects and is not related to a particular figure in the main text.

Supplementary Table 2 is related to Main Figure 3.

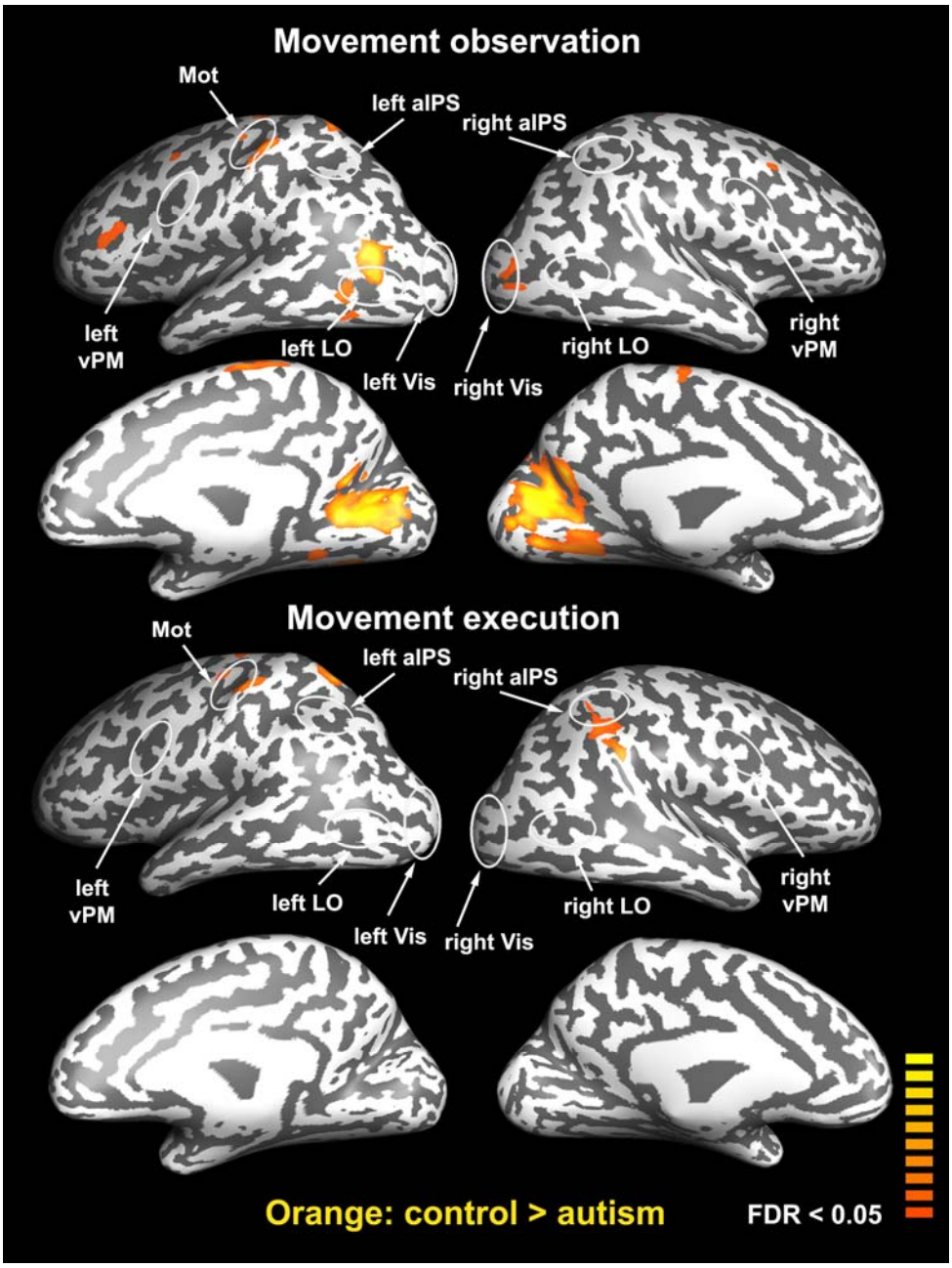

Supplementary Figure 1 (Related to main Figures 1 and 2): Cortical response differences between the two groups during movement observation experiment (top) and movement execution experiment (bottom). Orange: brain areas with significantly larger responses in the control group than the autism group. There were no brain areas that exhibited significantly larger responses in the autism group than the control group. White ellipses outline general location of the ROIs, which were selected separately for each subject. The prominent response difference between the two groups was in medial visual areas and in a left dorsal lateral occipital area, where control subjects exhibited significantly stronger responses than autistic subjects. Reducing the threshold of the analysis yielded noisy meaningless differences throughout the whole brain as well as in voxels outside the brain.

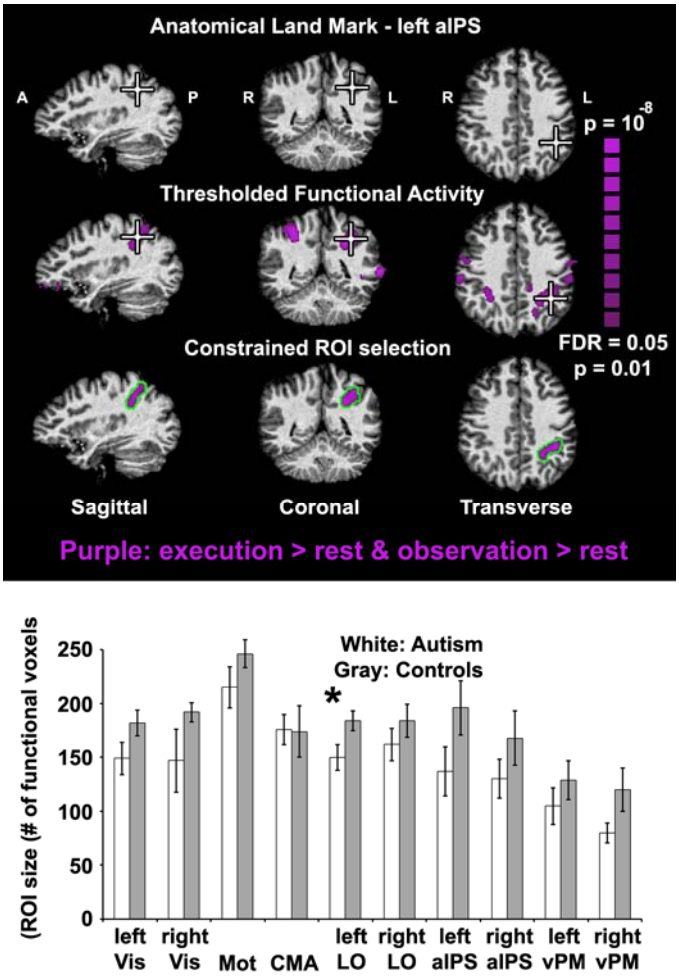

Supplementary Figure 2 (Related to main Figure 3): ROI Selection and size. **Top panel.** Selection of the aIPS ROI in an exemplar subject. First row: identifying the junction of anterior intraparietal sulcus and the post central sulcus as indicated by the cross-hairs. Middle row: overlaying voxels active during both execution and observation of movement (conjunction analysis - purple). Bottom row: selecting the ROI to include activated voxels within a maximum diameter of 15 mm^3 surrounding the anatomical landmark (outlined in green). **Bottom panel.** Average ROI size across individuals from the autism (white) and control (gray) groups. Error bars: Standard error of the mean. Asterisks: statistically significant difference ($p<0.05$, two tailed t-test, uncorrected to increase sensitivity). ROI sizes were generally larger in the control group, but significantly larger only in left LO.

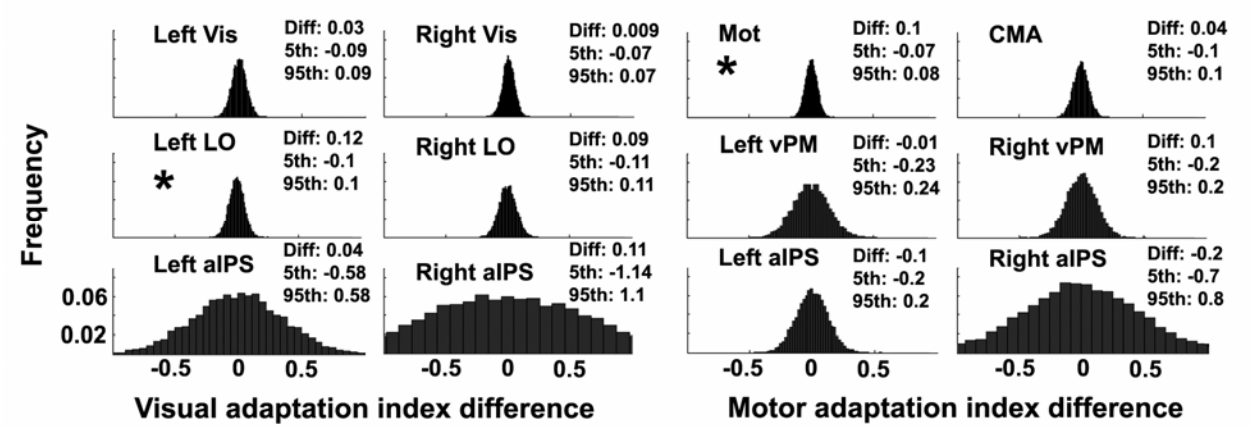

Supplementary Figure 3 (Related to main Figure 4): Randomized difference distributions of visual and motor adaptation indices. We used a randomization test to assess whether there was a significant difference in the amount of adaptation (adaptation index) exhibited by the autism and control groups in each of the relevant ROIs. We generated each distribution of index differences by randomly assigning individuals to either subject group (i.e., randomly shuffling subject identities). The randomization was repeated 10,000 times separately for each ROI to characterize ROI-specific randomized distributions. The resulting distributions describe the random differences found when comparing the visual and motor adaptation effects across such randomly assigned groups (i.e., according to the null hypothesis that there was no difference between groups). For the adaptation difference between the autism and control groups in a particular ROI to be considered statistically significant, it had to fall above the 95th percentile or below the 5th percentile of the relevant distribution. The widths of the distributions depended on how variable the adaptation indices were across individuals. For example, in early visual areas there was little variability among visual adaptation indices of both autistic and control subjects (Figure 4), creating a narrow distribution of index differences. Individuals with autism exhibited slightly stronger adaptation in left LO during the movement observation and in Mot during the movement execution experiment ($p > 0.05$). There was no statistically significant difference in the level of adaptation in any of the other ROIs.

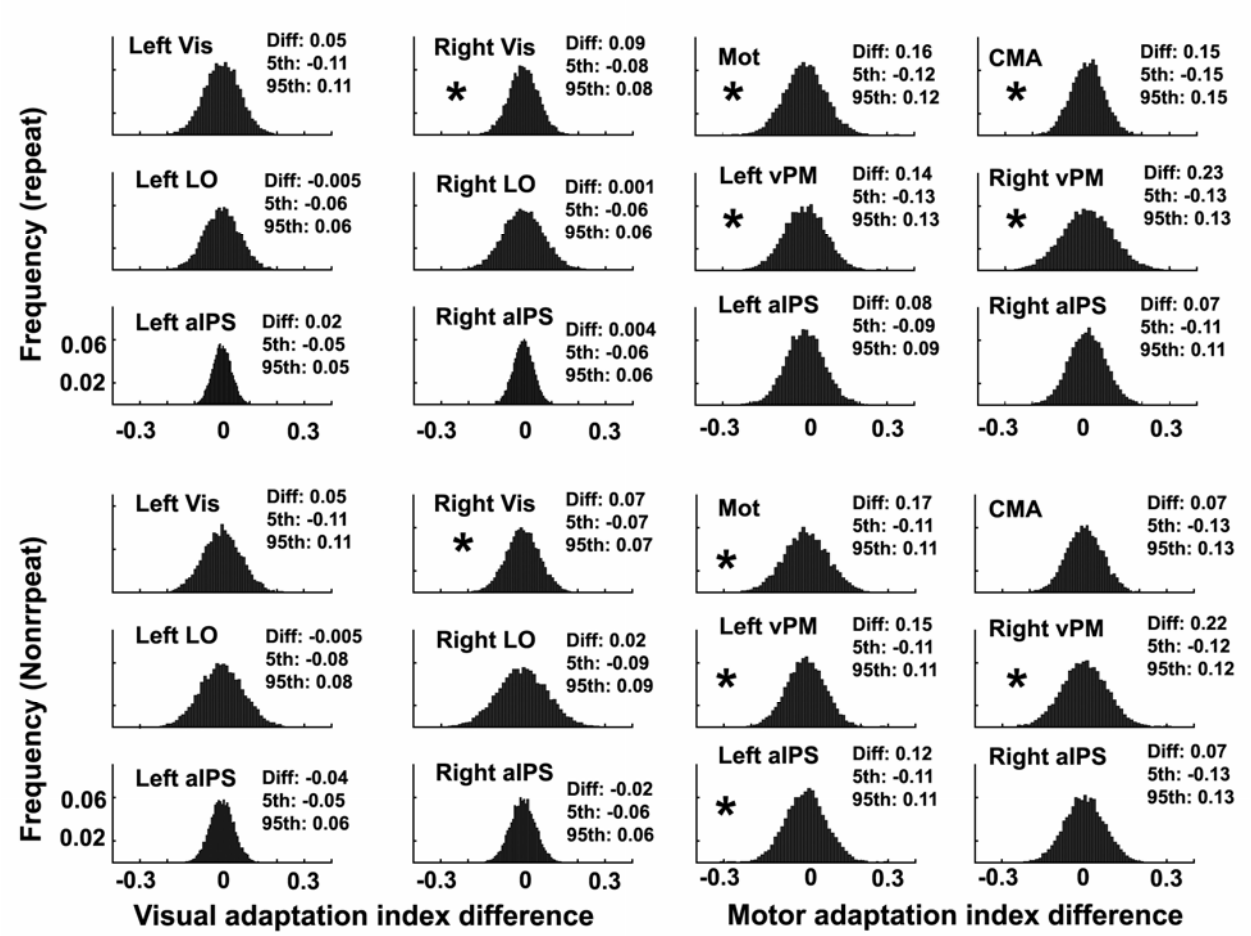

Supplementary Figure 4 (Related to main Figure 6): Randomized difference distributions of visual (left) and motor (right) standard deviations separately for repeat (top) and non-repeat (bottom) blocks (same format and procedure as Supplementary Figure 3). The resulting distributions describe the random differences found when comparing the visual and motor standard deviations across the randomly assigned groups (i.e., according to the null hypothesis that there was no difference between groups). The autism group exhibited significantly larger within-subject variability (larger standard deviation between blocks) in right Vis during the visual experiment and in Mot, CMA, right and left vPM, and left aIPS during the motor experiment ($p<0.05$).

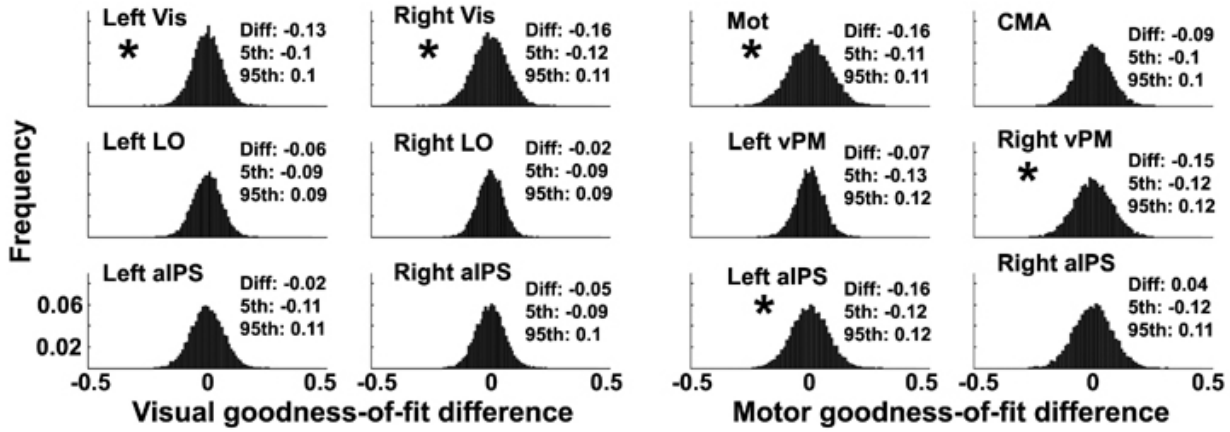

Supplementary Figure 5 (Related to main Figure 7): Randomized difference distributions of visual and motor model fits (same format and procedure as Supplementary Figure 3). The resulting distributions describe the random differences found when comparing the visual and motor model fits across the randomly assigned groups (i.e., according to the null hypothesis that there was no difference between groups). The autism group exhibited significantly larger within-subject variability (weaker model fits) in right and left Vis during the visual experiment and in Mot, right vPM, and left aIPS during the motor experiment ($p<0.05$).

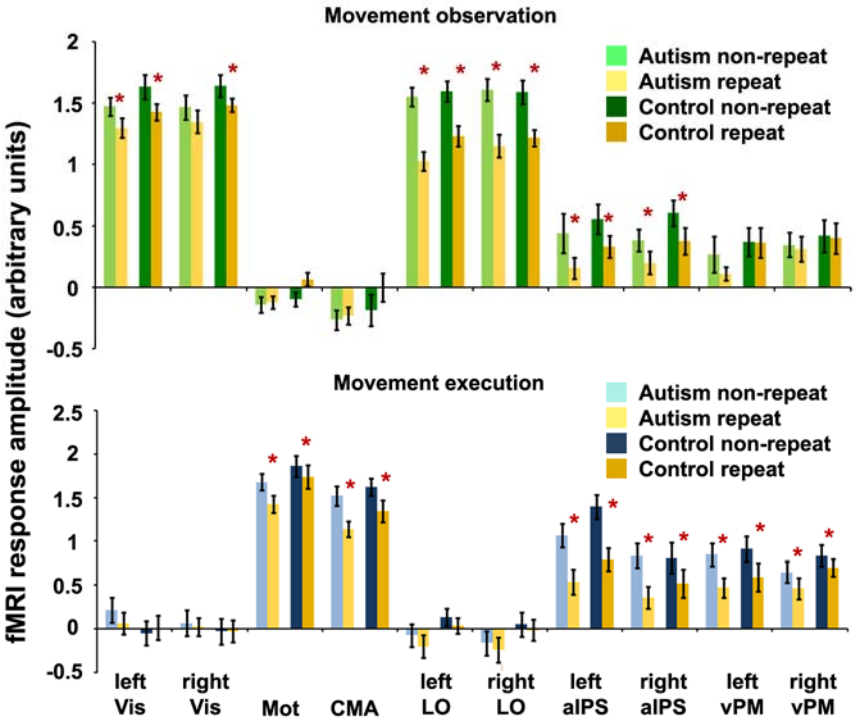

Supplementary Figure 6: Contracting the size of the original ROIs so that they were fixed to 100 functional voxels in all subjects of both groups revealed equivalent results (compare with Figure 3 - same ROI analysis). We identified the center voxel in each ROI of each subject and selected the closest 99 functional voxels from the original ROIs. In subjects where the original ROIs were smaller than 100 functional voxels we added neighboring voxels, equally distanced

from the center, so as to reach the same fixed ROI size across all subjects. Fixing the ROI size in this manner had negligible effects on the results. We re-computed the response amplitudes in each ROI for the visual (top) and motor (bottom) experiments and found significant adaptation in the same ROIs as reported before (Figure 3). Adaptation indices of the subjects also showed only minor differences and were equivalent to those reported in the main text (Figure 4). The conclusions regarding equivalent adaptation in both subject groups were, therefore, not dependent on the precise size of the ROIs and were equally evident when fixing the ROI size across all ROIs and all subjects.

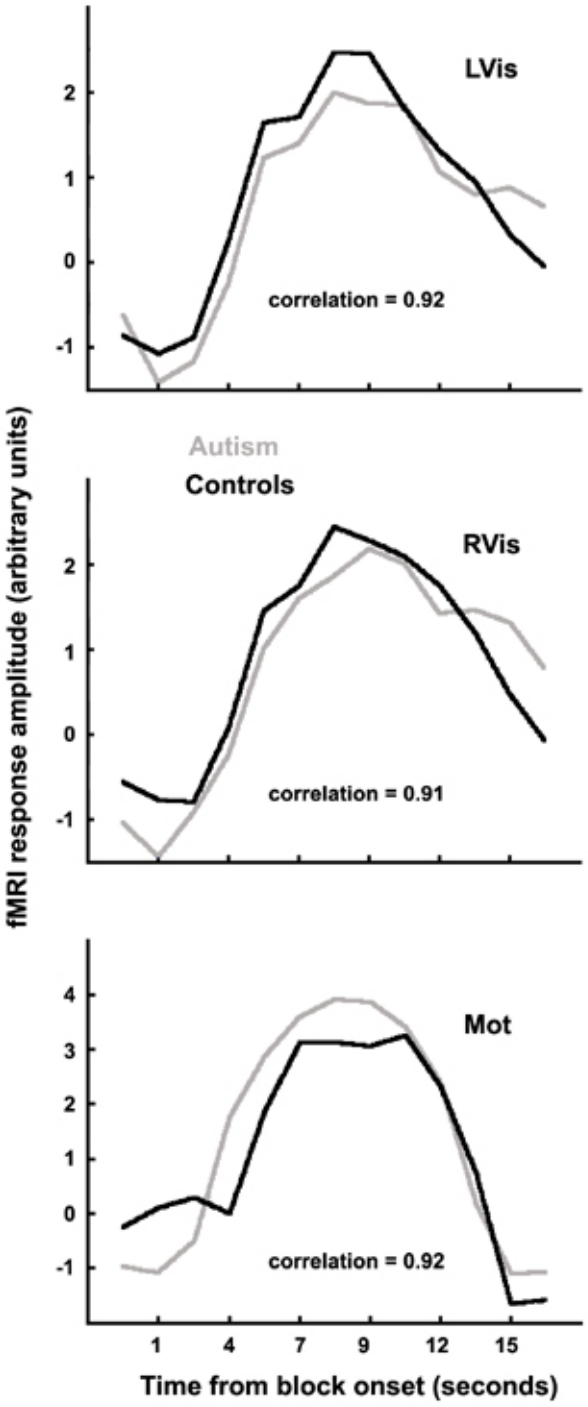

Supplementary Figure 7(Related to main Figures 5-7): Hemodynamic response functions (HRFs). The average deconvolved HRF across subjects with autism (gray) was almost identical to that of controls (black) as can be seen by the high correlation between the two. HRFs were calculated in left early visual areas (top) and right visual areas (middle) during the movement observation experiment and in primary motor and somatosensory areas (bottom) during the movement execution experiment.

To ensure that differences in the model fits were not due to systematic differences in the shape or duration of the HRFs of the two subject groups, we estimated an HRF individually for each subject using a “deconvolution” analysis. This analysis relied on linear regression, solving an equation of the form $\mathbf{y} = A\mathbf{x}$, where vector **y** was the measured fMRI time-course and vector **x** was the estimated individual-subject HRF containing 15 values. The model matrix *A* had 15 columns (corresponding to the number of time points in the estimated HRF). The first column of *A* contained a value of 1 at indices corresponding to the onset of movement blocks, the second column contained a 1 at indices corresponding to the second time point, and so on. Thus the model was made up of diagonals of 15 ones corresponding to every block where movements were observed/executed and zeros everywhere else. The result of this analysis yielded an individual HRF for each subject, which was averaged across subjects to determine the group’s HRF.

Age	VIQ	PIQ	IQ	ADI social	ADI communication	ADI stereotypy	ADOS social	ADOS communication
19	119	128	124	22	17	6	8	4
21	109	88	99	27	22	5	11	6
23	89	101	95	20	16	7	10	5
20	119	111	116	19	11	4	8	4
40	110	96	104	24	19	5	10	4
29	116	116	116	26	17	7	5	6
36	104	116	110	21	16	8	7	5
39	113	114	114	15	8	10	9	5
22	111	121	118	20	13	3	13	5
21	99	92	95	20	12	4	10	5

Supplementary Table 1: Age, IQ, ADOS, and ADI scores for the ten high-functioning autistic subjects included in this study.

ROI name	Talairach coordinates (x, y, z)					
	Autism			Control		
Left Vis	-12 (3.9)	-92 (2.2)	-0.1 (3.8)	-13(4)	-92 (2.1)	3 (7)
Right Vis	16 (4.3)	-88 (1.8)	1.8 (6)	16 (3.7)	-89 (2)	5.5 (5.4)
Mot	-38 (2.1)	-27 (3.2)	51 (1.2)	-37 (2.8)	-27 (3.3)	51 (1.2)
CMA	-2.3 (1.2)	-11 (4.6)	52 (3.3)	-2.5 (1.4)	-12 (3.6)	54 (3.6)
Left LO	-45 (2)	-70 (4)	1 (4.8)	-44 (3)	-71 (5.4)	1 (4.3)
Right LO	42 (4.2)	-65 (5.7)	-2.8 (3.9)	42 (3.5)	-66 (5.9)	-2.5 (3.5)
Left aIPS	-36 (3.9)	-44 (4.4)	47 (3.7)	-36 (4.2)	-46 (6.2)	46 (3.7)
Right aIPS	37 (3)	-42 (4.6)	46 (2.8)	35 (4.4)	-43 (4.9)	45 (3)
Left vPM	-49 (5.7)	3.8 (3.6)	27 (4.8)	-49 (3.8)	5 (5.3)	27 (5)
Right vPM	48 (2.8)	5.2 (4.4)	26 (4.3)	46 (4.5)	6.8 (4.8)	30 (4)

Supplementary Table 2 (Related to main Figure 3): Mean ROI location across subjects. Talairach coordinates (mean x, y, and z center of mass) are listed for each ROI along with the standard deviation in parentheses. The anatomical landmarks used to identify the ROIs were: occipital poles for right and left early visual areas (left and right Vis), the “hand knob” landmark in left central sulcus for primary motor and somatosensory cortex (Mot), the middle of the

cingulate sulcus medial to the central sulcus for cingulate motor area (CMA) the anterior ends of the lateral occipital sulci for lateral occipital areas (left and right LO), the junction of the intraparietal sulcus and post central sulcus for anterior intraparietal sulci (left and right aIPS), and the junction of inferior frontal sulcus and precentral sulcus for ventral premotor areas (left and right vPM)